Temperature dependence in interatomic potentials and an improved potential for Ti

G.J.Ackland

School of Physics, JCMB, The King's Buildings, University of Edinburgh, EH9 3JZ.

E-mail: gjackland@ed.ac.uk

Abstract. The process of deriving an interatomic potentials represents an attempt to integrate out the electronic degrees of freedom from the full quantum description of a condensed matter system. In practice it is the derivatives of the interatomic potentials which are used in molecular dynamics, as a model for the forces on a system. These forces should be the derivative of the free energy of the electronic system, which includes contributions from the entropy of the electronic states. This free energy is weakly temperature dependent, and although this can be safely neglected in many cases there are some systems where the electronic entropy plays a significant role. Here a method is proposed to incorporate electronic entropy in the Sommerfeld approximation into empirical potentials. The method is applied as a correction to an existing potential for titanium. Thermal properties of the new model are calculated, and a simple method for fixing the melting point and solid-solid phase transition temperature for existing models fitted to zero temperature data is presented.

1. Introduction

Classical molecular dynamics simulations are widely used in many areas of the physical sciences. Eliminating the explicit treatment of electronic degrees of freedom brings a computational advantage of around six orders of magnitude in the simulation of metallic systems, large enough to tackle systems which would be crippled by finite size effects in an electronic structure calculation. For applications in microstructure, plasticity and radiation damage where one wishes to study the behaviour of the atoms rather than electronic structure, this makes classical MD the method of choice.

The price for this is that the interatomic forces must be represented by the derivative of an interatomic potential, which is necessarily a poor approximation to the electronic structure. Typically this potential involves some functional form fitted to empirical or *ab initio*-calculated data. It is useful to distinguish the two distinct sources of error involved in this process: incorrect functional form and poor fitting.

Many MD simulations are still conducted using a pairwise-additive interatomic potential, such as Lennard Jones or Coulomb charges. Such pairwise potentials constrain possible values of the elastic constants. Most notably, the "Cauchy" relation which relates C_{12} with C_{66}. In a pairwise potential, elastic constants are given by the second derivative of the energy with respect to strain. Regarding the potential as a function of r^2 rather than r, it is easy to show that for *any* pair potential:

$$C_{12} = C_{66} = \frac{2}{\Omega} \sum_{ij} V''(r_{ij}^2) x_{ij}^2 y_{ij}^2$$

where r_{ij}, x_{ij}, y_{ij} are the separation between atoms i and j, and x,y components thereof. where i, j run over all atoms and Ω is the volume of the system. Experimentally, this is true only for strongly ionic materials. Table 1 shows that elasticity in NaCl can be described by pairwise forces, but it is impossible to fit the three independent elastic constants for typical oxides, noble gases, water and metals. No amount of fitting can circumvent this mathematical constraint: the problem is one of of incorrect functional form.

Table 1. Elastic constants for selected materials showing the violation of the cauchy relation $C_{12} = C_{66}$ and by implication the impossibility of describing these materials by a pairwise additive potential. For water the constants are C_{13} and C_{44}, the hexagonal equivalent relation

Material	C_{11}	C_{12}	C_{66}
NaCl	482	128	127
MgO	291	96	152
Argon	233	149	117
SiC	385	135	257
Cu	168	121	75
Fe	237	141	116
Water ice		59	31

There are many similar examples where an incorrect functional form renders the process of fitting impossible. About 25 years ago there was a strong move away from pairwise forces, in particular in metals, in favour of models which describe the local environment such as the Embedded atom method[3], Finnis-Sinclair[2], and Tersoff[4]. Easily justified by elementary consideration of the electronic structure, these functional forms allowed enough freedom in fitting to avoid the Cauchy constraint and similar relations governing surface and vacancy energies. They satisfy the needs of most applications, and even if transferrability is imperfect have remained the workhorse of atomistic simulation ever since.

Some more recent potential developments have simplified the fitting process or made it more intuitive. The Modified Embedded Atom Method[5] maps local coordination onto spherical harmonics and hence establishes a link to electron orbitals. Two band and magnetic potentials[6, 7, 8] explicitly introduce limited electronic degrees of freedom, and then show how to eliminate them analytically, leaving a simple potential of embedded atom form, but justifying more complicated parameterisations.

Ultimately, however, derivation of a functional form for a potential should go back to first principles. The overwhelming success of the Kohn-Sham formulation of the density functional theory suggests that we should start with the Kohn-Sham Hamiltonian[9], which in standard notation is:

$$F(\rho) = T[\rho] + \frac{1}{2}\int \frac{\rho(\mathbf{r})\rho(\mathbf{r}')}{4\pi\epsilon_0|\mathbf{r}-\mathbf{r}'|} d^3\mathbf{r} d^3\mathbf{r}' + E_{xc}[\rho] + \sum_i \int \frac{Z_i e \rho(\mathbf{r}')}{4\pi\epsilon_0|\mathbf{R_i}-\mathbf{r}'|} d^3\mathbf{r}' + \sum_i \sum_j \frac{Z_i Z_j e^2}{4\pi\epsilon_0|\mathbf{R_i}-\mathbf{R_j}|} \tag{1}$$

For molecular dynamics we are interested in forces. These can be calculated using the Hellmann-Feynman theorem[10] which tells us that the forces are simply the *partial* derivative of the Kohn-Sham Hamiltonian with respect to ionic positions R_i. Inspection of eq.1 shows that only the final two, electrostatic, terms contribute to this.

At finite temperature the electron free energy for a metal changes as the Fermi distribution becomes non-singular. The energy increases as states above the Fermi are occupied, while the

electronic entropy also increases due to partial occupations. According to Sommerfeld theory[11] there is an additional temperature-dependent contribution to the free energy which depends on temperature and the density of states at the Fermi energy as

$$F_{som}(T) \propto T^2 n(E_F)$$

In many electronic structure packages this effect is exploited to improve the numerical stability of the self consistency loop, by calculating with finite temperature electrons, so-called "Fermi Smearing". Typical effective temperatures can run to thousands of Kelvin, and the result is adjusted back to zero Kelvin. Nevertheless, the Sommerfeld temperature dependence of the electronic free energy is real, and so any potential involving integrating out electronic degrees of freedom should itself be temperature dependent. It is worth recalling at this point that the Hellmann-Feynman theorem is valid only for an electronic energy which is a *variational minimum* with respect to the parameters describing the electronic structure. For the Fermi-smeared system the variational quantity is the electronic *free energy* ($U_{el} - TS_{el}$), so the Hellman-Feynman forces are the derivative of this. The physical assumption underlying this is similar, though not identical, to the Born-Oppenheimer approximation: the ionic motion should be slow enough for the electrons to relax into their equilibrium distribution.

The temperature dependence of the Sommerfeld electronic free energy for Ti is shown in Fig.1 alongside the associated density of states. These figures were calculated using the CASTEP[13] program with settings as given in previous work[1], using Fermi-Dirac smearing with the smearing width corresponding to the quoted temperature. In all cases the atoms were located on their ideal lattice sites. The density of states was calculated using the *castepdos* program, which interpolates and integrates the density of states using the octahedron method between the explicitly calculated k-points.[14] At 0.05eV (about 600K) the Sommerfeld contribution in bcc is 34meV compared with 7meV for hcp. This is about 20% of the free energy difference at 0K.

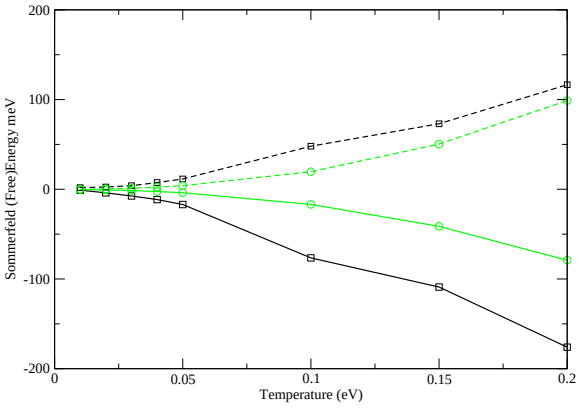

Figure 1. Sommerfeld electronic energy (dashed lines) and free energy (solid lines) for bcc (black, squares) and hcp (green, circles) Ti

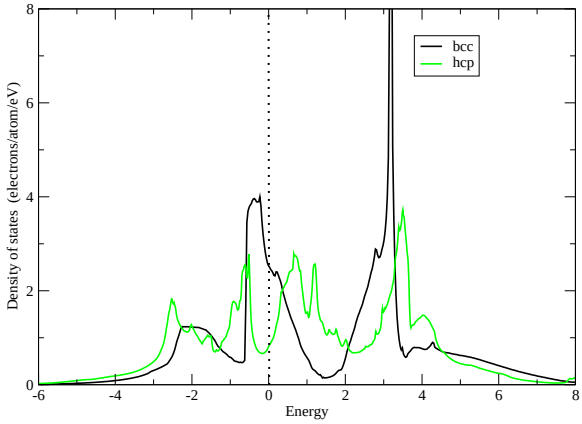

Figure 2. Density of states for bcc (black) and hcp (green) Ti

2. Sommerfeld Potentials

In order to include Sommerfeld effects in molecular dynamics, the potential must be written in the form of a sum of energies per atom j in an arrangement of atoms i in positions $\{\mathbf{r_i}\}$:

$$U(\{\mathbf{r_i}\}) = \sum_j U_0(\mathbf{r_j}, \{\mathbf{r_i}\}) + F_{som}(\mathbf{r_j}, \{\mathbf{r_i}\}) \quad (2)$$

The vast majority of interatomic potentials are fitted to (extrapolated) zero-temperature experimental data and/or *ab initio* data calculated on the Born-Oppenheimer surface. Thus in many cases good parameterisations for U_0 already exist. Here we consider the second term in equation 2, which is proportional to T^2. The proportionality constant can be treated as a fitting parameter (A_T). The challenge is to obtain a sensible measure for the local density of states at the Fermi energy $n_j(E_f)$ in terms of the atomic positions without performing a full electronic structure calculation. The most convenient approach is to write it as a pairwise function:

$$n_j(E_f) = \sum_i f(|\mathbf{r_i} - \mathbf{r_j}|)$$

We could stop at this point, and simply take f as an arbitrary function to be fitted, however it is worth discussing how it might look.

2.1. Heuristics for f(r) in transition metals

$f(r)$ attempts to measure the density of states at the Fermi level projected onto an individual atom. This quantity can be readily calculated for various crystal structures (e.g. Fig 2), and may vary quite widely between them. If we consider a canonical d-band model, the density of states is very different between close-packed and bcc structures. The DoS can be defined in terms of moments, in particular the third and fourth moment determine the skew and kurtosis. The moments theorem[16] relates these to a real-space picture involving closed paths of near neighbour hops. This defines the key difference between close packing (many loops of three hops) and body centred cubic (no three-hop loops- many four loops). Open structures seldom feature in transition metals and their alloys, so we can neglect these.

Although counting paths of hops cannot be done directly by a pair potential, it suggests a related local measure. For practical purposes the skew/kurtosis relation can be approximated by using a function which is either sharply peaked around first neighbour (favours three-loop equilateral triangles) or a broader function which favours four-loops. Which is energetically favoured for a given material depends on the band filling.

In most existing EAM and Finnis Sinclair potentials this narrow vs broad minimum in the potential determines the stability of close packed vs bcc materials. In the moments picture, the longer range acts as a proxy for measuring four-membered rings. Use of exponential fitting functions, as in early EAMs, tends to give a narrow minimum; polynomial functions, as used in Finnis Sinclair potentials, give a broader minimum. This, rather than any deep physics, explains their early application to fcc and bcc respectively.

2.2. Application to Titanium

For titanium the Fermi level falls at a minimum of the hcp density of states, and a maximium of the bcc density of states. Thus we can expect that electronic entropy contributions will be different and significant in determining the phase transition temperature. Indeed, electronic entropy was shown to provide almost half the excess entropy of bcc Zr[12], a material very similar to Ti. The density of states is for valence electrons, so $f(r)$ should have significant value only outside the repulsive core. It is also desirable that its derivatives be continuous and the number of adjustable parameters is minimised. Consequently we write the function as:

$$f(r) = X^2(1-X)^2 \qquad 0 < X < 1; \qquad X = (r - r_o)/d$$

$$F_{som} = \sum_{ij} A_T T^2 X^2 (1-X)^2$$

this gives a three parameter model, defining the range of the interaction from r_0 to $r_o + d$ and the strength A_T

Most published potentials are fitted to zero temperature data, so this Sommerfeld term can simply be added. Moreover, the parameterisation is relatively straightforward: we have calculated the temperature-dependent contribution to the free energy for fcc and hcp Ti. These two pieces of data are sufficient to parameterise the model.

For Ti we consider a potential introduced in 1992[21] which is known to have too low a basal stacking fault but otherwise reproduces the behaviour of hcp titanium reasonably well. From Fig. 1 above we see that at low energies (up to 1000K) the Sommerfeld contribution to bcc is about 4.7 times that of hcp. This suggests an approximate solution $r_o = 2.84\mathring{A}$, $d = 1.46\mathring{A}$, $A_T = -7.5 \times 10^{-7} meV/K^2$.

2.3. Which temperature to use?

In order to use the temperature-dependent potential, it is necessary to specify the electronic temperature. In practice, most MD simulations are relatively small and one can assume that the electrons are able to reach thermal equilibrium throughout the region.

Thus for an NVT/NPT calculation run using a thermostat, one can simply use the thermostat temperature to fix a constant potential throughout the run. For NVE one can use the instantaneous global temperature of the simulation for all atoms, so although the potential may vary in time, it is constant across space.

3. Tests of the new potentials

To test the thermal effects we have carried out melting point calculations from bcc and hcp Ti, and thermal expansion calculations.

3.1. Melting Point Calculations

We determined melting point using the coexistence method[18], using the MOLDY program in the NPE ensemble[17]. By using intermediate sized systems, 16000 and 13824 atoms for hcp and bcc respectively, it is possible to suppress the bcc-hcp transition and calculate melting points from both hcp and bcc phases. The original potential[21] gives a melting point of 1395 ± 10K (hcp) and 1790 ± 10 K (bcc), the difference indicating the stability of bcc at high temperature. This contrasts with the 0K energies of -4.853eV (hcp) and -4.807eV (bcc) which indicate low temperature stability of hcp. The transition at intermediate temperature is via a soft phonon analogous to zirconium[12, 15], and care must be taken to ensure that the solid phase does not transform during the simulation, which we did by monitoring local coordination using the BallViewer code[19].

Experimentally, the melting temperature of Ti is 1941K, and the bcc-hcp transition is at 1155 K. The original potential therefore gives too low a melting temperature. The effect of the Sommerfeld correction on the melting is small (1315K and 1800K), slightly stabilising bcc and destabilising hcp.

Metals melt at high temperature because the liquid phase has higher entropy than the solid. Thus the more of the phase space the system can reach without too high potential energy, the lower will be the melting point. Since a melt samples interatomic distances shorter than typically realised in the solid, softening the potential inside nearest neighbour distances can be expected to favour the liquid. In the present potential, the a_6 spline parameter controls the short range repulsion. The 1992 potential was not fitted to any data for short-ranged interactions, and in Fig. 3 we show the evolution of the melting temperature as a function of the parameter a_6: the short ranged spline starting close to nearest neighbour separations (see Appendix A). The effect on the melting point is very pronounced, while the 0K properties are essentially unaffected.

The original potential had $a_6 = 0.494\text{eV}/\text{Å}^3$: the experimental melting point (1941K) and ab initio hcp-bcc difference (90meV) were not fitted in 1992, and to do so requires a significantly stiffer short-ranged potential.

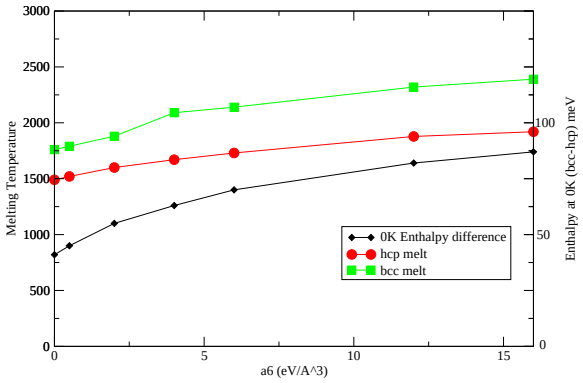

Figure 3. Effect of short ranged repulsion of melting point and zero-temperature hcp-bcc stability. See Appendix A for definition of a_6

3.2. Thermal Expansion

The thermal expansion is not typically fitted in empirical potentials, and in consequence is often significantly wrong. The Sommerfeld correction introduces additional temperature-dependent anharmonicity into the potential, which affects the thermal expansion. For this potential the thermal expansion is close to the experimental data but highly temperature dependent, especially at high temperature where the softening around second neighbours leads to high values.

3.3. Phase Transformation Calculations

Whatever value is used, the Sommerfeld correction will be insufficient to reduce the enthalpy of bcc below hcp: the bcc structure is always stabilised by phonon entropy. The constraints imposed by the crystal symmetry mean that it is not possible to calculate the phase transition temperature between hcp and bcc by coexistence. Rather, it requires a full free energy calculation[20, 24] which can be performed by integrating using the Gibbs-Helmholtz equation:

$$\Delta(\frac{G}{T}) = -\int H/T^2 dT$$

The right hand side of this equation can be calculated from a single-phase NPT molecular dynamics calculation (see e.g. Appendix B), varying the temperature slowly by incrementing the required temperature of a Nose thermostat. In practice we use this equation with the two melting points and assume that H/T^2 varies linearly with T. The stabilising effect on bcc lowers the transition temperature considerably, the actual value depending on the chosen value of a_6.

Figure 4 shows the effect of the Sommerfeld potential in a dynamics calculation of the phase transition. Although this is only a lower bound for the thermodynamic transition temperature, it does illustrate the increased stability range of bcc.

4. Conclusions

The thermal excitation of electronic degrees of freedom introduces a temperature dependence into the electronic free energy. If the electronic degrees of freedom are integrated out to make an interatomic potential, this temperature dependence should remain. Where the excitation arises simply from the Fermi-Dirac distribution via Sommerfeld theory, this temperature dependence scales as T^2. The magnitude of the effect has been calculated for Ti using density functional theory, and found to give a contribution of a few tens of meV to the bcc-hcp free energy difference. This in turn is enough to lower the calculated hcp-bcc phase transition temperature significantly,

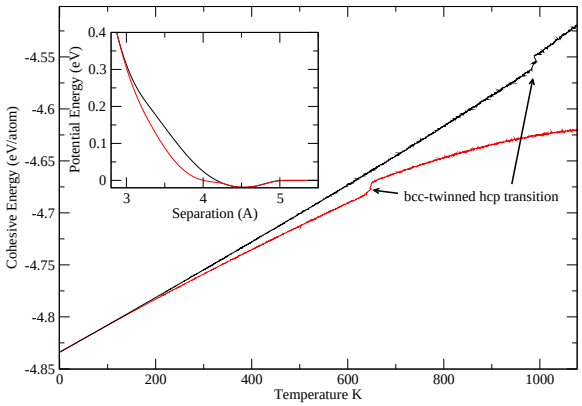

Figure 4. Plot of cohesive energy per atom vs temperature for MD simulation on heating with and without Sommerfeld correction. Main figure shows linear increase in energy with temperature, as expected from virial theorem (original potential, black line). Corrected potential (red) shows deviation from virial behaviour as electronic degrees of freedom are excited at high T. Both cases have a discontinuity as the cooling bcc transforms to twinned hcp, the correction stabilises bcc, dropping the observed transformation from 1000K to 650K. Inset shows pair potential V(r) at 0K and 1250K .

but has less effect on the melting temperature. Neither effect is large compared to the errors of typical EAM-type potentials which do not include melting temperature as a fit parameter.

By contrast, the melting temperature has strong correlation with the short ranged part of the potential, inside the normal separations found and fitted at 0K. By adjusting only the short-range terms it is possible to refit the melting point of a potential fitted to elastic moduli, cohesive energy, vacancy and surface formation etc. without disturbing those properties. This suggests a simple way to improve the high temperature phase performance of existing potentials without major redevelopment[26, 27, 28]. Note that energies of self interstitials[2, 3, 7] and interstitial impurities[14, 29] may be affected.

In addition to Sommerfeld correction, a strong temperature dependence of the electron free energy may be found in magnetic materials such as iron[30, 31, 32], where the fcc phase is stabilised by paramagnetic free energy. This effect could be captured by a temperature-dependent potential, although the excitation of all magnetic modes means the temperature dependence would be more complex, requiring an additional many-body term rather than a pairwise one. This will be the subject of future work.

5. Appendix A

The potential has a functional form for the energy of the i^{th} atom

$$U_i = \sum_j \sum_k H(r_k - R_{ij}) a_k (r_k - R_{ij})^3 \quad (3)$$

$$\sum_j A_T T^2 X^2 (1-X)^2 H(r_o + d - R_{ij}) H(R_{ij} - r_o) \quad (4)$$

$$- \sqrt{\sum_j \sum_k H(R_k - R_{ij}) A_k (R_k - R_{ij})^3} \quad (5)$$

with X as defined above, R_{ij} the separation between i^{th} and j^{th} nearest atoms, H the Heaviside step function and the other parameters given inTable A1 below.

k	1	2	3	4	5	6
a_k	-0.785715	1.110966	-0.299450	-0.143061	1.025368	0.494293
r_k	5.09113	5.00767	4.673828	3.964408	3.338449	2.9508
A_k	0.547614	-0.551266				
R_k	5.09113	4.381714				
	$A_T = -7.5\times10^{-7}$	r_o=2.84	d=1.4			

Table 2. Table A1. Parameters for the Ti potential, from ref.[21], converted into units of eV and Angstroms, and for the temperature-dependent correction. Note that a_6 can be varied to fit th

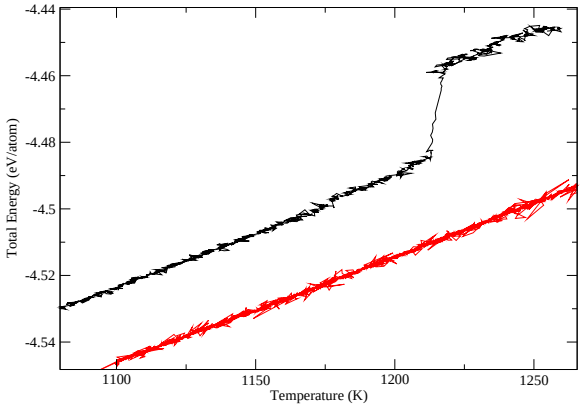

Figure 5. Plot of enthalpy vs temperature showing failure of thermodynamic integration due to phase transition from bcc to deformed hcp on cooling. Upper line (black) is bcc at high temperature, transforming to twinned hcp on cooling. Reheating gave hysteresis in the retransformation. Note the different transuition point compared with fig 4. Lower line (red) is hcp on heating from 0K: recooling produced the same curve. NPT simulations were run with a cooling rate of 1K/ps and a 1fs timestep, with a Nose relaxation time parameter of 100fs. Phases were initialised in a supercell with periodic boundaries compatible with the phase in question: although the transformation could happen in principle in Parrinello-Rahman dynamics, in practice the transformation is slow enough to gather phonon statistics.

6. Appendix B

One potential drawback of the thermodynamic integration is that the system will undergo a phase transformation as the temperature is varied, rather than remaining in the metastable phase. When this occurs, the latent heat causes a discontinuity in a graph of enthalpy vs temperature. Fig.5. shows an example of this in cooling of the bcc phase. Some authors have maintained that if the transformation occurs quickly enough, the temperature of the discontinuity would be the transformation temperature. However, better statistics than are available here are needed to ensure that this is so[25]. Moreover, Fig 5. shows that the transformation is not to the pure hcp phase, and BallViewer analysis[19] shows that the low temperature phase is a twinned hcp.

7. References

[1] B.E.Tegner, L. Zhu, and G.J. Ackland Phys.Rev.B (2012)
[2] Finnis,M.W. and Sinclair,J.E., Phil.Mag.A, 50, 45. (1984)
[3] Daw,M.S. and Baskes,M.I., Phys.Rev.B 29, 6443 (1984)
[4] J.Tersoff, Phys.Rev.Lett. **56**, 632 (1986)

[5] M.I.Baskes, Phys Rev B, 46, 2727-2742 (1992)
[6] G.J.Ackland, S.K.Reed Phys Rev B 67 174108 (2003)
[7] Dudarev SL and Derlet PM J.Phys.CM, 19 239001 2007
[8] G.J.Ackland J.Nucl.Mater. 351, 1-3, 20 (2006)
[9] W.Kohn and L.J.Sham. *Phys.Rev.*, **140** 1133, (1965).
[10] Hellmann H (1937) *Einfuhrung in die Quantumchemie* (Leipzig: Franz Deutsche 1937); R. P Feynman, *Phys Rev* **56**, 340 (1939).
[11] N.W.Ashcroft and N.D.Mermin, Solid State Physics, Chapter 2.
[12] F.Willaime and C.Massobrio Phys. Rev. Lett. 63, 22442247 (1989)
[13] S.J.Clark, M.D.Segall, C.J.Pickard, P.J.Hasnip, M.J.Probert, K. Refson, M.C.Payne Zeitschrift fr Kristallographie 220(5-6) 567 (2005)
[14] G.J.Ackland, Phys.Rev.Letters, 80, 2233 (1998)
[15] U.Pinsook and G.J.Ackland, Phys.Rev.B 59 13642 (1999)
[16] F Cyrot-Lackmann J.Phys.Chem. Solids 29 1235 (1968)
[17] G.J.Ackland, K D'Mellow, S.L.Daraszewicz, D.J.Hepburn, M Uhrin and K.Stratford Comp.Phys.Comm., 182 2587 (2011)
[18] J.R.Morris, C.Z.Wang, K.M.Ho, and C.T.Chan Phys. Rev. B 49, 31093115 (1994)
[19] G.J.Ackland, and A.P.Jones Phys Rev B 73 054104 (2006)
[20] G.J.Ackland J.Phys.CM 14 2975 (2002)
[21] G.J.Ackland, Phil. Mag. A 66, 917-932 (1992).
[22] `\protect\vrule width0pt\protect\href{http://www2.ph.ed.ac.uk/\string~gja/dos/dos_manual}{http://www2.ph.ed.a`
[23] X.G. Lu M. Selleby, B. Sundman Calphad, 29 6889 (2005)
[24] E. M. Lopasso, M. Caro, A. Caro, and P. E. A. Turchi Phys. Rev. B 68, 214205 (2003)
[25] D. Alfe, C. Cazorla, and M. J. Gillan J. Chem. Phys. 135, 024102 (2011);
[26] R.C. Pasianot and L. Malerba J.Nucl.Mater. 360 118 (2007)
[27] Bonny G., Pasianot R. and Malerba L. Phil.Mag, 89 3451 (2009)
[28] J M Winey, A Kubota and Y M Gupta Modelling Simul. Mater. Sci. Eng. 17 055004 (2009)
[29] D.J.Hepburn and G.J.Ackland Physical Review B, 78, 16, 165115 (2008)
[30] H. Hasegawa and D. G. Pettifor Phys. Rev. Lett. 50, 130133 (1983)
[31] Hasegawa H, Finnis MW, Pettifor DG,J Phys F Met Phys, 17 2049 1987.
[32] P.-W. Ma, C.H. Woo, S.L. Dudarev, Phys. Rev. B78 024434 (2008)